International Journal of Mass Spectrometry 308 (2011) 289–298

Contents lists available at ScienceDirect

International Journal of Mass Spectrometry

journal homepage: www.elsevier.com/locate/ijms

Collision induced dissociation of protonated urea with N_2: Effects of rotational energy on reactivity and energy transfer via chemical dynamics simulations

Yannick Jeanvoine[a], Marie-Pierre Gaigeot[a,b,*], William L. Hase[c], Kihyung Song[d], Riccardo Spezia[a,**]

[a] LAMBE CNRS UMR 8587, Laboratoire Analyse et Modélisation pour la Biologie et l'Environnement, Université d'Evry-Val-d'Essonne, Bd. F. Mitterrand, 91025 Evry Cedex, France
[b] Institut Universitaire de France, 103 Blvd St Michel, 75005 Paris, France
[c] Department of Chemistry & Biochemistry, Texas Tech University, Lubbock, TX 79409, United States
[d] Department of Chemistry, Korea National University of Education, Chungbuk 363-791, South Korea

ARTICLE INFO

Article history:
Received 22 May 2011
Received in revised form 25 July 2011
Accepted 26 July 2011
Available online 4 August 2011

Keywords:
Collision induced dissociation
Energy transfer
Gas phase reactivity
Molecular dynamics
Rotational energy
QM/MM chemical dynamics

ABSTRACT

In the present work we have investigated the gas phase reactivity of protonated urea after collision with the diatomic inert gas N_2, by studying the energy transfer and fragmentation induced by collisions. We first developed an analytical pair potential to describe the interaction between the projectile and the ion, and then performed QM/MM direct chemical dynamics simulations of the collision between the projectile and protonated urea in its two most stable isomers. In particular, the effect of the diatomic projectile, and the role of its initial rotational state, were compared with the fragmentation and energy transfer obtained previously (*J. Phys. Chem. A* 2009, *113*, 13853) for the monoatomic projectile Ar. The diatomic projectile was found to be less efficient in energy transfer compared to the monoatomic projectile. In addition, rotational activation of $UreaH^+$ is dependent on the initial rotational quantum number of N_2. Finally, we investigated the $UreaH^+$ gas phase reactivity as a function of its rovibrational activation by means of chemical dynamics simulations where the initial structure for the simulations is the transition state (TS) that the system can reach after collisional activation of the most stable isomer. The simulation time-length is not able to directly access this TS from the most stable isomer since its lifetime is notably longer, of about two order of magnitude in time.

1. Introduction

Collision-induced dissociation (CID) is an important experimental method to study structure and reactivity of a variety of molecular systems, including small molecules [1–3], clusters [4–7], and organic [8–10] and biological molecules [11–15]. In CID, an ion is energised by collisions with a noble gas atom or unreactive molecule such as N_2. In the limit of low energy collisions, electronic excitation is unimportant and the collisions transfer a fraction of the translational energy to vibrational/rotational energy of the molecular ion so that it can eventually dissociate. It is possible to monitor the residual parent and product ions after CID.

Recently, we studied CID of protonated urea by coupling chemical dynamics simulations, RRKM analysis and ESI-MS/MS experiments. In particular we found that, after energy transfer to $UreaH^+$, fragmentation to high energy products occurred, resulting from either non-RRKM effects and/or dynamics driven by the high rotational energy of $UreaH^+$ [16]. In this first study we investigated collisions with Ar, for which an analytic interaction potential was previously developed by Meroueh and Hase [17]. We employed a QM/MM method for the simulations, where the projectile–ion interaction was represented by the above analytic pair potential (MM), while the ion was treated at the MP2 level (QM) in order to allow the system to dissociate.

In many MS/MS experiments N_2 is used as inert collision gas, mainly because of the lower cost compared to noble gases. This gas has a mass higher than Ne and smaller than Ar, but it is often assumed to behave similarly. A detailed study on the effect of the projectile on CID, limited to noble gases, was performed by Anderson and co-workers [18], who demonstrated that Ne, Ar and Kr behave similarly and only Xe leads to a different CID efficiency. N_2, while in the same mass range of "light" noble gases, has internal degrees of freedom and its rotational energy may play a role in energy transfer.

Chemical dynamics simulations [19] can model CID processes by calculating an ensemble of trajectories for which the projectile ion and the inert gas collide with a given relative translational energy and all possible relative collision orientations present in CID

* Corresponding author at: LAMBE CNRS UMR 8587, Laboratoire Analyse et Modélisation pour la Biologie et l'Environnement, Université d'Evry-Val-d'Essonne, Bd. F. Mitterrand, 91025 Evry Cedex, France.
** Corresponding author.
E-mail addresses: mgaigeot@univ-evry.fr (M.-P. Gaigeot), rspezia@univ-evry.fr (R. Spezia).

1387-3806/$ – see front matter © 2011 Elsevier B.V. All rights reserved.
doi:10.1016/j.ijms.2011.07.029

experiments are sampled [20]. In the case of a diatomic projectile such as N_2, its initial rotational state must also be chosen according to the Boltzmann distribution. At room temperature its vibration is in the ground state. This simulation method, which requires hundreds or thousands of trajectories for statistical relevance, can be done by using an analytic [21] potential energy function or by direct dynamics [22]. For some special cases it is possible to use an analytic function which includes unimolecular decomposition paths for the ion [21], but more common is to use a molecular mechanical (MM) potential for the ion, which does not describe unimolecular decomposition. The latter yields the efficiency of translation-to-vibration (T → V) and translation-to-rotation (T → R) energy transfer in CID [23]. With direct dynamics a quantum mechanical (QM) model is used for the ion and decompositions, which occur during the simulation time-length [22], can be studied. *Ab initio* direct dynamics for CID become very computationally expensive as the size of the ion grows and, thus, it can be useful to treat only the ion by QM and use MM potentials for interactions with its collision partner [23].

An interaction potential of the same (or similar) form as that used previously for Ar/UreaH$^+$ was not available for N_2/UreaH$^+$ and, thus, was first derived in the present study. With this potential we studied energy transfer and reactivity, finding that the rotational energy of a projectile plays an important role. Only one isomer of protonated urea is able to react within the simulation time-length; i.e., there is not sufficient time for the more stable isomer to reach the isomerisation transition state and then eventually react. From energy transfer obtained from the simulations for the more stable isomer, we initiated trajectories from this transition state with the appropriate rotational and vibrational energies. Rotational energy was found to be crucial in determining the reactivity.

2. Computational details

2.1. Potential energy function

The general analytic potential energy function used for the N_2 + UreaH$^+$ system is represented by

$$V = V_{\mathrm{UreaH}^+} + V_{\mathrm{N_2}} + V_{\mathrm{N_2/UreaH}^+} \quad (1)$$

where V_{UreaH^+} is the UreaH$^+$ intramolecular potential represented by MP2/6-31G* *ab initio* calculations (as in Ref. [16]), $V_{\mathrm{N_2}}$ is the N_2 intramolecular potential and $V_{\mathrm{N_2/UreaH}^+}$ is the intermolecular potential between the projectile (N_2) and the ion (UreaH$^+$). For the latter two terms we employed analytical pair potentials, whose parameters were obtained from *ab initio* calculations as detailed in the following.

The N_2 intramolecular stretching potential is harmonic, where the equilibrium distance (1.12 Å) and vibrational frequency (2176 cm^{-1}) were obtained from MP2/6-311++G** calculations. The N_2/UreaH$^+$ interaction potential is a sum of two-body terms of the form:

$$V_{N-i} = ae^{-br_{N-i}} - \frac{c}{r_{N-i}^9} \quad (2)$$

where r_{N-i} is the distance between each nitrogen atom of N_2 and each atom, i, of UreaH$^+$. This interaction potential expression is the same as the one used and parametrized by Meroueh and Hase for Ar-Peptide CID and recently used by us in QM/MM direct chemical dynamics simulations of Ar-UreaH$^+$ and Ar-[Ca(Urea)]$^{2+}$ [16,24]. Atom–atom parameters were obtained by fitting interaction energy curves obtained from QCISD(T)/6-31++G** calculations with BSSE corrections by employing the counterpoise method [25,26], i.e., the same level of theory as employed in Ref. [17].

To obtain the two-body parameters in Eq. (2), we divided UreaH$^+$ into building blocks, similarly to what was done to obtain parameters for Ar CID simulations of protonated polyglycines [17], where the NH_3, NH_4^+, CH_4 and HCO_2H building blocks were used. The molecules NH_3, NH_4^+, and formic acid were used as the building blocks for UreaH$^+$. For N_2 interacting with each of these molecules, different orientations of both N_2 and the molecules were considered.

Table 1
Intermolecular potential parameters.[a]

Potential	a	B	C
N_2/NH_3 (N_2N)	60,253.8	5.56	0.76
N_2/NH_3 (N_2H)	968.1	1.83	0.15
N_2/NH_4^+ (N_2N)	42,545.1	4.81	1.10
N_2/NH_4^+ (N_2H)	5040.2	3.70	0.02
N_2/HCO_2H (N_2OH)[b]	20,393.7	4.02	3.16
N_2/HCO_2H (N_2HO)	6263.5	4.46	0.17
N_2/HCO_2H (N_2CO)	1344.4	1.41	45.89
N_2/HCO_2H (N_2OC)	19,520.2	4.07	3.27
N_2/HCO_2H (N_2HC)	10,268.5	5.38	0.00

[a] Parameters for Eq. (2) with a, b, and c in units of kcal/mol, Å^{-1}, and kcal Å^9/mol, respectively.
[b] Two-body potential between N_2 and an oxygen atom of the OH group of a carboxylic acid group.

The potentials between N_2 and the N and H atoms of an amine group were determined from N_2/NH_3 *ab initio* calculations, which are shown in Fig. 1. The potential curves are for N_2 interacting with NH_3 front-side and back-side, along the C_{3V} axis, and interacting on the side, with different rotational orientations of N_2, as shown in the same Fig. 1. The interaction between N_2 and the atoms of the protonated amine end group was modelled by interactions of the N_2 and the ammonium molecule. As for the above N_2/NH_3 *ab initio* calculations, N_2/NH_4^+ interactions were calculated for both front-side and back-side C_{3V} interactions, with different N_2 rotational orientations. The *ab initio* and fitted curves are plotted in Fig. 2. The two-body interaction potentials between N_2 and the atoms of a carboxylic group were determined from four sets of *ab initio* calculations for the N_2/formic acid system. Intermolecular potentials were calculated for interactions along the O–H···N_2, C=O···N_2, and N_2···C=O axes and for N_2 interacting with the O atom of OH along an N_2···O axis parallel to the C=O bond (see Fig. 3). Also in this case different N_2 rotational orientations were considered. The potential energy curves for these calculations are given in Fig. 3.

The parameters of Eq. (2) were obtained by simultaneously fitting all the potential energy curves for each system studied. The resulting fits are plotted in Figs. 1–3, and it is seen that there is globally good agreement between the *ab initio* and fitted curves. The potential parameters derived for the two-body potentials are listed in Table 1.

2.2. Collision induced simulations

Two Urea-H$^+$ structures were considered for the direct dynamics simulations: one protonated on oxygen (OPr) and one on nitrogen (NPr), with their geometries optimized at the MP2/6-31G* level of theory (see Fig. 4). As discussed in our previous work [16], the potential energy minimum of NPr, calculated with MP2 using the 6-31G* and aug-cc-pVTZ basis sets, is 9.7 and 13.8 kcal/mol higher in energy, respectively, than that of OPr, corresponding to 9.0 and 13.4 kcal/mol free energy differences, respectively. Thus, for thermal equilibrium conditions there is negligible population of the NPr isomer. However, ESI experiments are likely to be non-equilibrium for small systems as reported by several studies [27–30]. Consequently, there may be a substantial population of NPr. Thus, we considered both isomers, OPr and NPr (as previously done for Ar collisions [16]) for the work presented here, which allow us to compare with the results obtained for the monoatomic projectile Ar.

Initial conditions for each UreaH$^+$ isomer were chosen by adding a quasi-classical 300 K Boltzmann distribution of

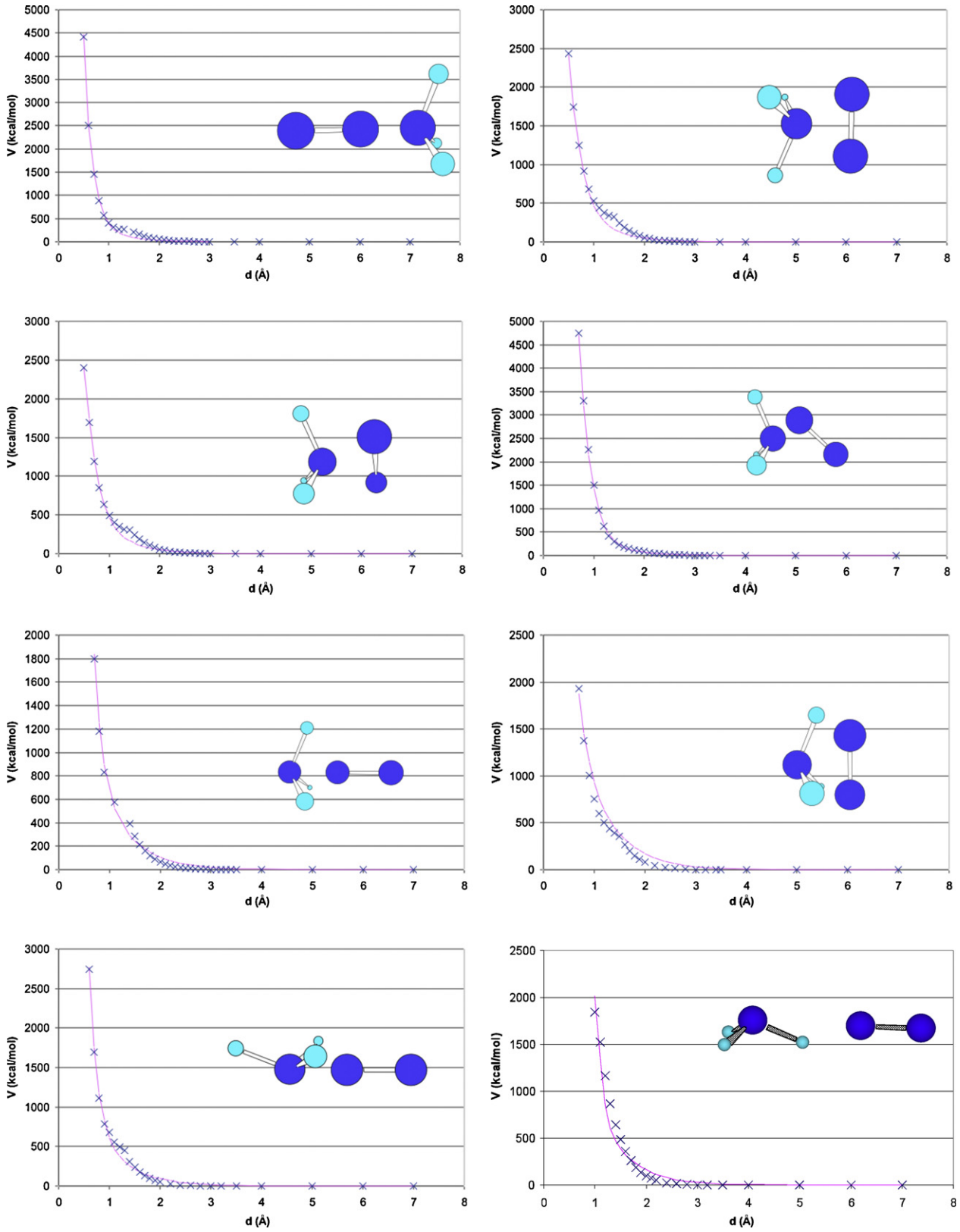

Fig. 1. *Ab initio* (crosses) and fitted Eq. (2) (solid lines) potential energy curves for $N_2 + NH_3$.

vibrational/rotational energies about the isomers' potential energy minima [31–33]. Energies for the normal modes of vibration were selected from a 300 K Boltzmann distribution. The resulting normal mode energies were partitioned between kinetic and potential energies by choosing a random phase for each normal mode. A 300 K rotational energy of RT/2 was added to each principal axis of rotation for the isomers. The initial rotational energy of the projectile N_2 was set accordingly to its initial rotational quantum number. For N_2 at 300 K the spectrum of accessible J varies in a 0–20 range, according to the Boltzmann distribution. We thus selected three

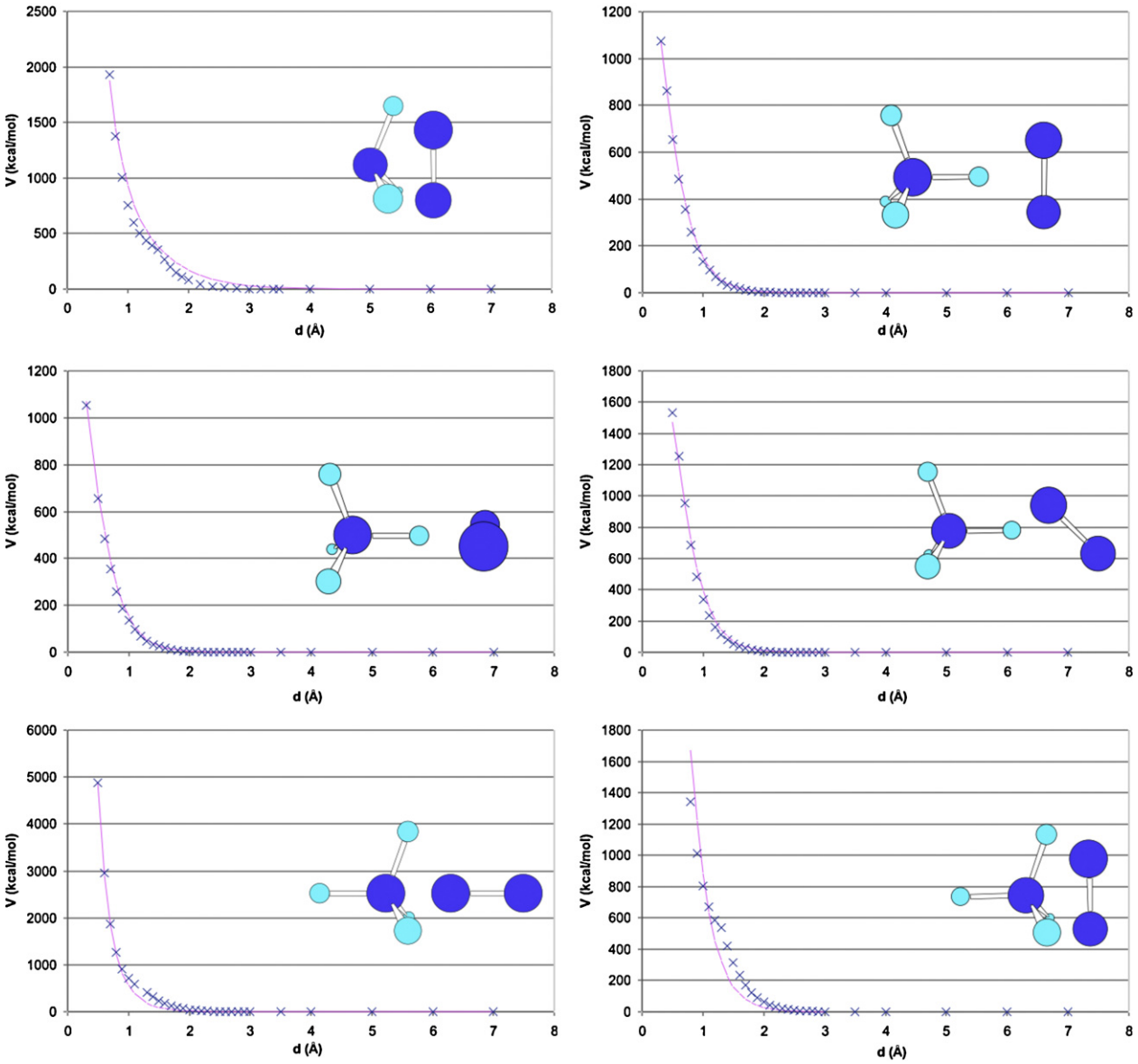

Fig. 2. *Ab initio* (crosses) and fitted Eq. (2) (solid lines) potential energy curves for $N_2 + NH_4^+$.

initial rotational energies corresponding to three quantum numbers that are representative of that distribution, i.e., $J = 2$, 7, and 14.[1] N_2 was put into its ground vibrational state.

The vibrational and rotational energies of the UreaH$^+$ isomer and N_2 were transformed into Cartesian coordinates and momenta following well-known algorithms implemented in VENUS [34,35]. The isomer and N_2 were then randomly rotated about their Euler angles to take into account the random directions of the N_2 + UreaH$^+$ collisions. The relative velocity was then added to N_2 + UreaH$^+$ in accord with the center-of-mass collision energy and impact parameter. A collision energy of 145.1 kcal/mol was considered, corresponding to the higher (and most reactive) energy considered in the Ar collision work [16]. The impact parameter, b, was chosen randomly between 0 and b_{max}. The latter was fixed to the value of 3.0 Å from geometrical considerations and because we noticed that collisions with larger values of b did not transfer sufficient energy to fragment UreaH$^+$. This value was reduced to 2.5 Å for the OPr simulations since, as shown in Section 3, no fragmentations were observed in the CID simulations using OPr as the starting structure.

The trajectories were calculated using a software package consisting of the general chemical dynamics computer program VENUS96 [34,35] coupled to Gaussian 03 [36]. The latter was used to calculate the potential energy and gradient for the UreaH$^+$ intramolecular potential. The classical equations of motion were integrated using the velocity Verlet algorithm [37] with a time step of 0.2 fs that gives energy conservation for both reactive and nonreactive trajectories. The trajectories were initiated at an ion–projectile distance of 7.0 Å, large enough to guarantee no interaction between the ion and the colliding atom. Simulations with the OPr isomer were halted at a distance of 12 Å, corresponding to about 250 fs simulation time, that is enough to guarantee no interactions between N_2 and the ion at the end. For the NPr isomer this halting distance was extended up to 50 Å, corresponding to a

[1] $J = 7$ corresponds to the maximum of the rotational quantum numbers Boltzmann distribution at 300 K, $J = 2$ and $J = 14$ are chosen as two limit values to understand the low and high N_2 initial rotational energy limits. In the case of liquid nitrogen temperature, the distribution is shifted to lower values and the maximum is now for $J = 3$.

simulation time-length of about 0.6 ps, to give the system enough time to eventually react (while for OPr we have already shown [16] that reaction does not occur within the time length of the *ab initio* chemical dynamics trajectory). A trajectory was stopped if the ion dissociates. In that case, the criterion distance of 7.0 Å was also used to guarantee no interactions between fragments. For each OPr simulation, we performed 130 trajectories for each initial rotational quantum number of the projectile ($J = 2$; 7; 14). For the NPr simulations we performed 350 trajectories with $J = 7$ each of about 0.6 ps in length. To obtain an understanding of the role of the initial N_2 rotational quantum number on the NPr reactivity, we performed simulations with $J = 2$ and 14 (90 trajectories in each case) where

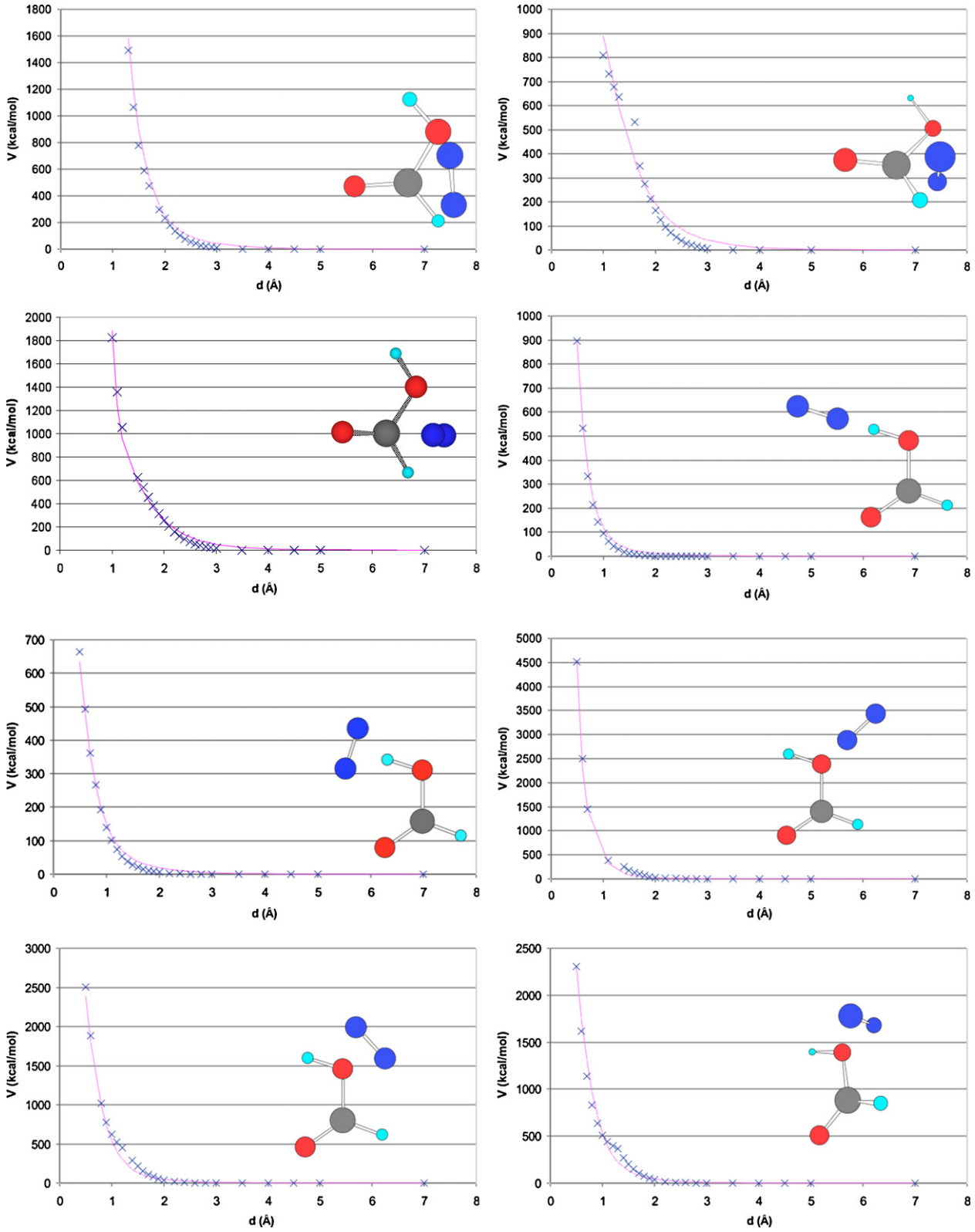

Fig. 3. *Ab initio* (crosses) and fitted Eq. (2) (solid lines) potential energy curves for $N_2 + HCO_2H$.

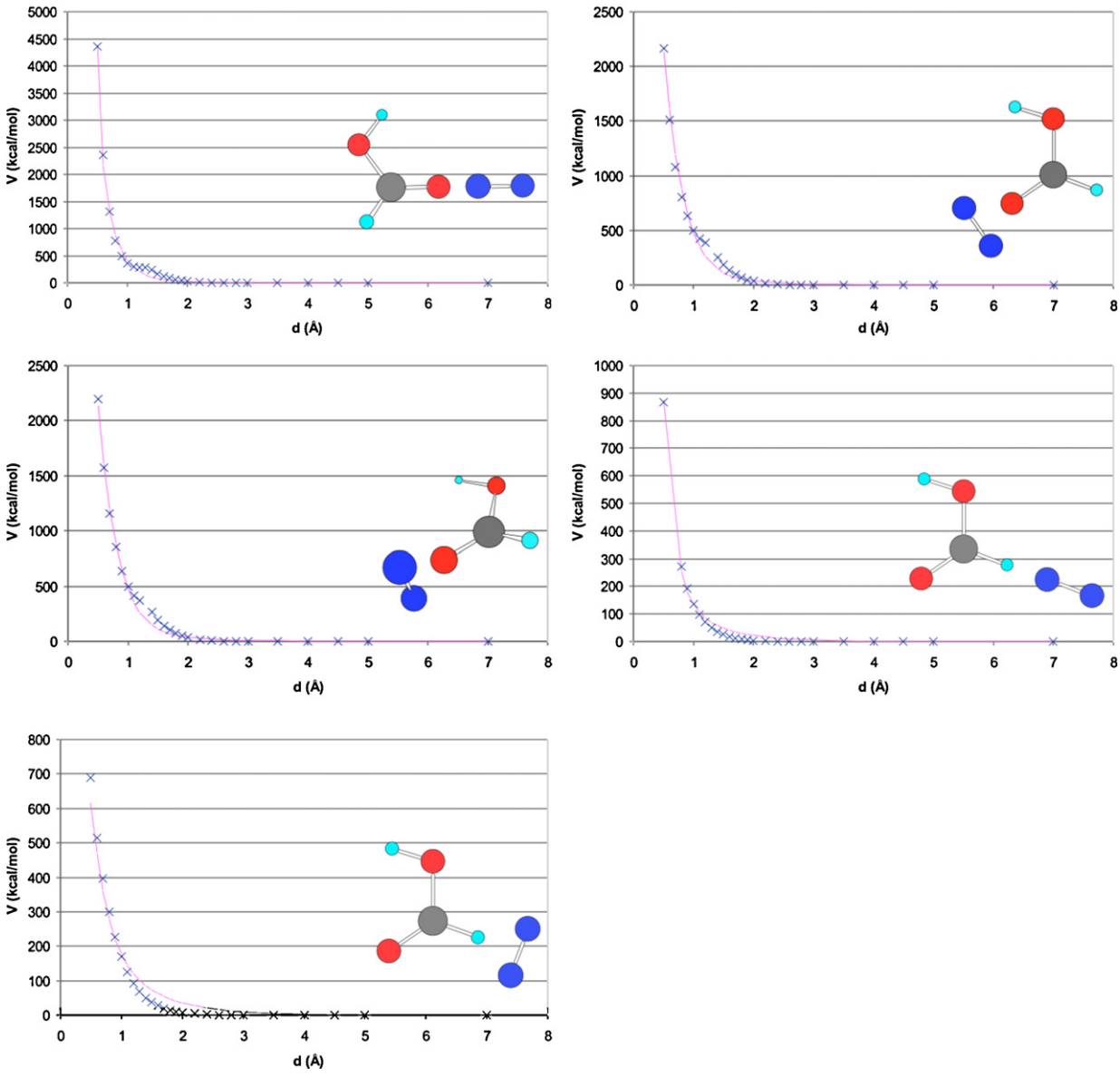

Fig. 3. (*Continued*).

the system is halted when the N_2-ion distance is larger than 20 Å, corresponding to roughly 350 fs of simulation time. A simulation with the same condition was also performed for $J = 7$ in order to compare results with the same simulation time-length for all the J values.

2.3. Saddle point trajectories

The two minima for the $UreaH^+$ potential energy surface, OPr and NPr, are connected through a transition state (TS) corresponding to proton transfer from the oxygen to nitrogen site (Fig. 4). This TS is reachable after CID activation of the OPr isomer, with a barrier of about 41 kcal/mol (this corresponds to proton transfer coupled with NH_2 rotation as described in our previous work [16]), but not in the time-scale accessible by the QM/MM chemical dynamics simulations (the isomerisation occurs in the 10–1000 ps range as determined by a previous RRKM analysis) [16]. However, the CID reactivity may be studied by investigating the reaction paths obtained using as a starting point this TS and giving it vibrational and rotational energies consistent with

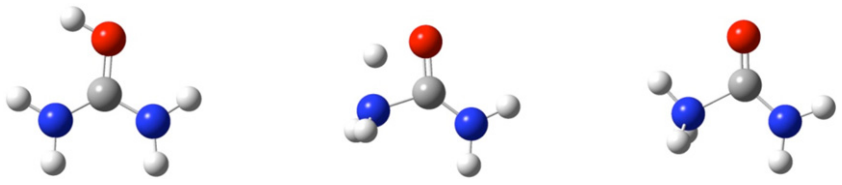

Fig. 4. The three protonated urea structures used as initial structure for the chemical dynamics simulations. OPr (left) and NPr (right) are used in the CID simulations, while the TS (middle) was used to study reaction pathways from the energised TS.

the CID activation. Here, we have chosen internal vibrational and rotational energies that are within the range obtained from the chemical dynamics simulations. We have considered three activation vibrational energies (where the zero corresponds to the OPr isomer) of 55, 65 and 75 kcal/mol, corresponding to energies 14, 24 and 34 kcal/mol higher than the TS barrier, respectively. Also, two rotational activation energies of 20 and 50 kcal/mol were considered. For each initial condition, we ran about 140 independent trajectories from the TS structure, for a maximum time-length of about 2.0 ps per trajectory. A trajectory is stopped if a fragmentation occurs, using the same distance criteria used before (see Section 2.2). The procedure for selecting initial conditions for these trajectories has been described previously [38].

The above direct chemical dynamics simulations were done by employing VENUS96 [34,35] coupled with Gaussian 03 [36], where the $UreaH^+$ potential energy surface is obtained on the fly at the MP2/6-31G* level of theory.

3. Results

3.1. Energy transfer

As found in our previous Ar + $UreaH^+$ study [16], all trajectories with the OPr initial structure do not react in the available time-length. Also, the majority of the trajectories with the NPr initial structure (here we consider those for N_2 with its most probable rotational quantum number $J = 7$) do not react (68.8%), that is considerably higher (lower reactivity) with respect to what was obtained with the same relative collision energy for the Ar projectile (44.2%) [16].

In Fig. 5 we show the vibrational, rotational and total energies of protonated OPr after collision with N_2 at different initial rotational quantum numbers. We should first note that energy transfer to OPr for both vibration and rotation is lower with respect to what was obtained with Ar for the same collision energy. This reduces both the vibrational and the rotational energy of OPr. Comparing the percentage of trajectories that have enough vibrational energy to pass the TS (i.e., trajectories with more than 40 kcal/mol of vibrational energy after collision),[2] we should note that while for Ar we found 9% of the trajectories sufficiently energised [16], for N_2 this percentage decreases to 2% for $J = 2$ and $J = 7$ (and 0% for $J = 14$). Note that the final rotational energy of the activated ion shows a dependence with the initial rotational state of the projectile N_2. This is shown clearly in Fig. 6 where we present a scatter plot between vibrational and rotational energies of OPr as a function of the initial N_2 rotational quantum number. Note that such high fractions of the collision energy transferred to rotational energy have been found in previous simulations of the collisional activation of peptides [39], of planar Al clusters [40], and for the previous Ar + $UreaH^+$ study [16].

As we have already discussed in our previous work [16], rotational energy should not have a big effect in promoting the OPr isomer to TS, but, as is shown in the following, it can have an important role in the subsequent fragmentation dynamics.

3.2. Reactivity

Gas phase protonated urea fragmentation can proceed through two pathways:

path 1 : $UreaH^+ \rightarrow NH_3 + CONH_2{}^+$

path 2 : $UreaH^+ \rightarrow NH_4{}^+ + OCNH$

where path 1 provides products higher in energy than those of path 2 by about 30-35 kcal/mol. For sake of clarity here and hereafter we

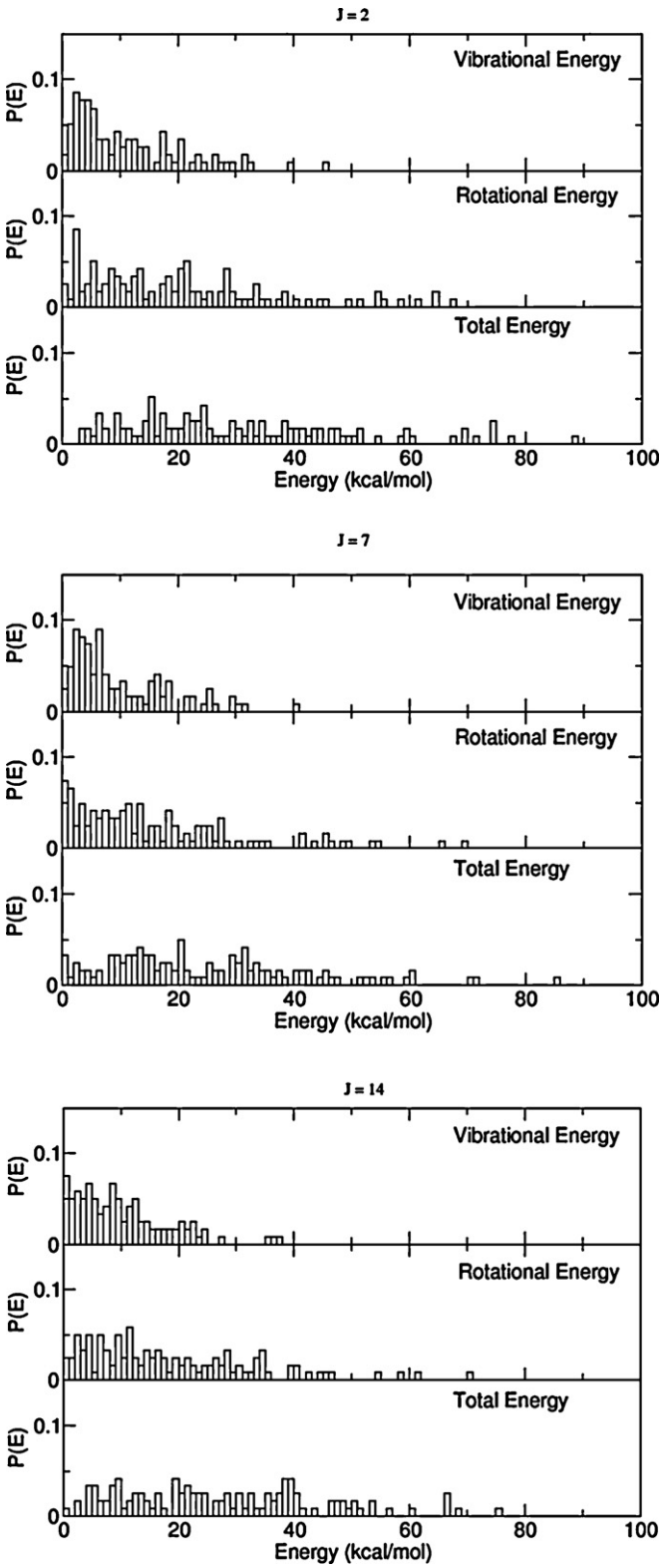

Fig. 5. Nonreactive OPr trajectories' vibrational, rotational and total energy distributions, following collisions with N_2 for the three initial rotational quantum numbers of the projectile. The collision energy is 145.1 kcal/mol.

[2] The full potential energy curve for $UreaH^+$ gas phase reactivity is described in details in Ref. [16] and depicted in Fig. 3 of the same article.

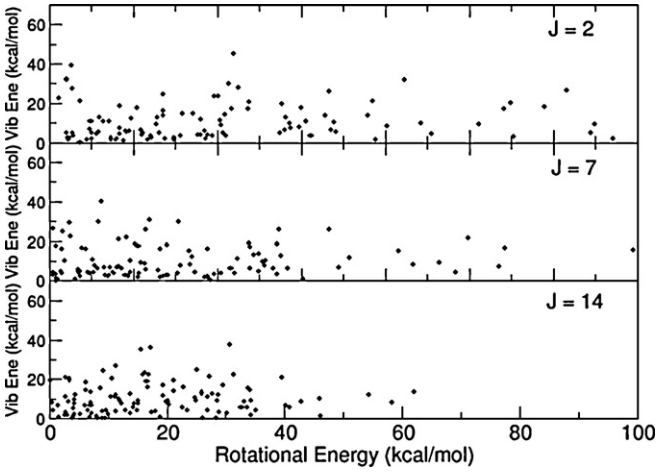

Fig. 6. Scatter plot of rotational versus vibrational energy of OPr obtained from nonreactive N_2 + OPr trajectories for the three initial rotational quantum number of the projectile. The collision energy is 145.1 kcal/mol.

refer to NH_3 for path 1 and NH_4^+ for path 2 (it is implied that we have both products for the reactions forming NH_3 and NH_4^+).

When the CID chemical dynamics simulations are performed using the NPr isomer as the initial structure (here we consider long trajectories corresponding to the most probable $J = 7$ rotational quantum number of N_2), 31% of the trajectories are able to react in the investigated time-length. Inspecting the reactive trajectories, we obtain the percentage of the two possible reaction paths and the mechanisms that lead to each product. In particular, we distinguish two possible mechanisms: a "shattering" mechanism, where following NPr collisional activation the C–N bond is broken just after one vibrational period and an internal energy transfer mechanism (ET), where this happens in more than one vibrational period (this does not necessarily entail full IVR). The same distinction between these two mechanisms was done in our previous study with the Ar projectile [16], such that we can compare results, as summarised in Table 2. As expected from the lower energy transfer obtained by using N_2, the NPr reactivity is also lowered for N_2 as compared to Ar. The NH_3/NH_4^+ product ratio of 0.63 for N_2 is higher than the value of 0.18 for Ar at the same relative energy, mainly due to the lower probability of obtaining NH_4^+ (19% with N_2 and 37% with Ar). The probability of forming NH_3 has a smaller decrease; i.e., 12% for N_2 vs 19% for Ar. Looking at details of the reaction dynamics shows that the shattering mechanism is much less probable for N_2, as expected [16], since the shattering/ET ratio increases as energy transfer increases.

The initial rotational quantum number of N_2 seems to play a role in determining the total reactivity, since for $J = 2$ there are 10% more reactive trajectories than for $J = 7$ and $J = 14$. This is in agreement with the finding of a higher energy transfer for the $J = 2$ initial conditions. Collisions obtained from simulations where N_2 is initially in the $J = 2$ rotational state are able to transfer more energy

Table 2
Reactivity (in percentage) after collision of the NPr isomer from chemical dynamics simulations.

	N_2[a]	Ar[b]
No reaction	69	44
NH_3/shattering	4	17
NH_3/ET[c]	8	2
NH_4^+/shattering	10	24
NH_4^+/ET[c]	9	13

[a] This study for $J = 7$.
[b] From Ref. [1].
[c] ET is for energy transfer mechanism.

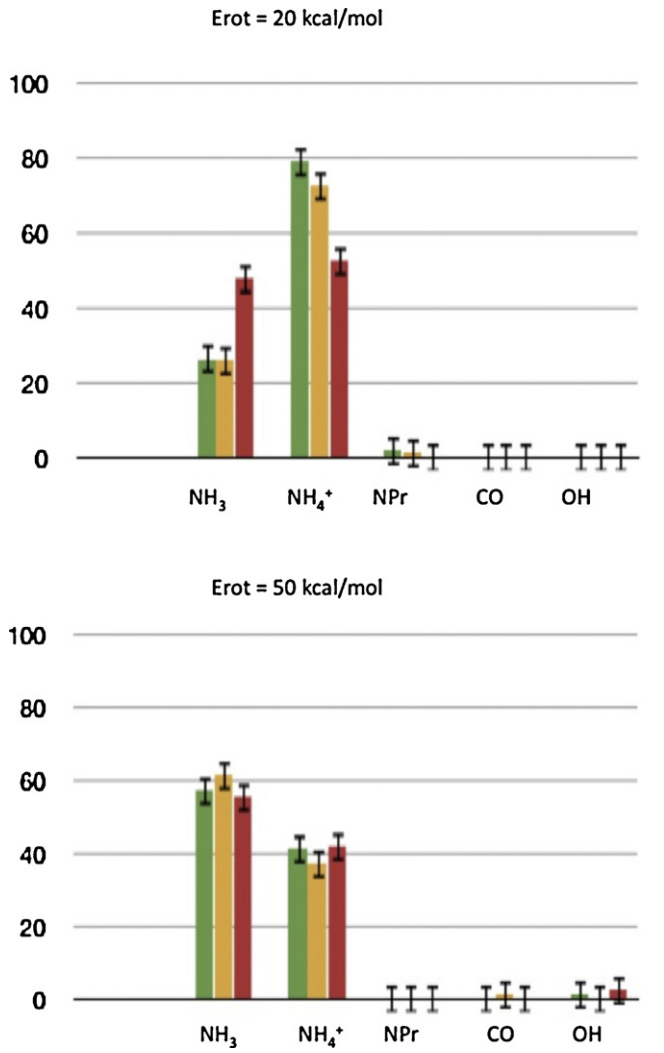

Fig. 7. Products probability distributions (in %) for trajectories initiated at the OPr ↔ NPr TS at two different rotational energies (upper panel 20 kcal/mol, lower panel 50 kcal/mol). In each case the three vibrational activation energies are 55 (green), 65 (yellow), and 75 (red) kcal/mol. The green column is on the left, the yellow column in the middle, and the red column is on the right. (For interpretation of the references to colour in this figure legend, the reader is referred to the web version of the article.)

(vibrational and in particular rotational) and then break the C–N bond more easily, obtaining more NH_3 and NH_4^+ products than for $J = 7$ and $J = 14$. This supports the conclusion that that rotational activation of $UreaH^+$ is important to drive the systems towards fragmentation pathways.

The reactivity obtained directly from the CID chemical dynamics simulations of the NPr isomer corresponds to the situation where the NPr isomer is formed and thermalised during the electrospray ionization process and then collides with neutral N_2 in the collision cell. From the $UreaH^+$ PES we know that this is not the most stable isomer. We have thus investigated another dynamical limit for $UreaH^+$ reactivity for which the system in its more stable isomer (OPr) acquires rotational and vibrational energy from collisions and reaches the transition state between OPr and NPr. From this TS the system dynamically evolves either towards the products (fragments or NPr) or it goes back to reactant (OPr). Thus, we follow this evolution by means of chemical dynamics simulations. We have investigated two rotational energies (20 and 50 kcal/mol) and three vibrational energies (55, 65 and 75 kcal/mol) in order to see the effect of the internal energy distribution at the TS on the reactivity. In Fig. 7 we report the percentage of products obtained from

chemical dynamics simulations starting from the TS, as a function of the vibrational and rotational energies given to the ion. Since the sign of the reaction coordinate translational energy is chosen randomly, approximately 50% of trajectories go back to OPr.

By inspecting the products obtained, we find that increasing the rotational energy of $UreaH^+$ increases the NH_3 products and concomitantly decreases the NH_4^+ products. In particular, while for a low rotational energy NH_4^+ is the most abundant product, NH_3 is the most abundant one for the high rotational energy. Note that NH_4^+, corresponding to path 2, is the most stable in energy. This means that rotational activation is able to bring the system towards a fragmentation pathway leading to high energy products. This result confirms that rotational activation is fundamental for forming the high energy product NH_3 from $UreaH^+$ dissociation, as was proposed in our early study [16]. For each initial TS rotational energy, increasing the vibrational energy increases the formation of NH_3, a result consistent with the higher barrier for NH_3 formation as compared to NH_4^+ formation. A higher vibrational excitation increases the probability of attaining the higher energy products.

Finally, we found some other species as minor products (less than 2% as shown in Fig. 7) for the trajectories initiated at the TS. They are NPr, CO and OH. Since the system has a high energy for the trajectories initiated at the TS, NPr is rarely seen as a product since it rapidly dissociates to NH_3 or NH_4^+. CO and OH are obtained only at high TS activation energies (both rotational and vibrational) and are not observed in either the CID simulations or experiments. The loss of neutral CO would correspond to m/z 23 while for OH we can have a neutral (and radical) loss that will provide m/z 44 (the same as NH_3 lost), or the negative ion loss that would generate a doubly charged cation m/z 22 for a positive mode detector. Experiments do not provide any m/z 22 and 23 clear peaks and only some noise is observed in this region [16].

4. Conclusions

In this work we have studied the CID of protonated urea by employing a diatomic molecule, N_2, as a projectile in order to investigate differences that can be obtained in reactivity when such an inert gas is used in mass spectrometry experiments instead of a monoatomic noble gas like Ar. This molecular gas is largely employed in mass spectrometry experiments due to the lower cost of N_2 as compared to rare gases. For this aim we have developed an interaction potential between N_2 and atoms present in $UreaH^+$. This was done using the same procedure previously adopted for Ar [17] and, in addition, it provides an interaction potential that can be used to study CID simulations of other related systems (for instance peptides) with N_2 as the collision gas.

Both reactivity and energy transfer (comparing results for the same ion with the same relative collision energy) seem to be lower in the case of a diatomic projectile in comparison to our previous results for a mono-atomic projectile [16]. The rotational energy transfer to $UreaH^+$ is also function of the initial rotational quantum number J of the N_2 projectile. A higher J leads to a lower rotational activation of the ion. There are several possible physical origins of this effect. One are the different interaction times between projectiles with low and high rotational energy (and J). Low J may result in a longer interaction time and thus shorter average interacting distance. In terms of Mahan's model [41] this corresponds to a larger range parameter and thus more energy transfer. Conversely, for high J the projectile rotates more with a smaller interaction time and thus has a larger average interaction distance (and thus less energy transfer). The transfer of rotational energy to $UreaH^+$ must be done within the constraint of constant total angular momentum J and this may be less probable as the initial angular momentum j_{N_2} of N_2 is increased. The total angular momentum is the vector sum $J = j_{N_2} + j_{UreaH^+} + l$, where l is the orbital angular momentum. The reactivity of $UreaH^+$ follows the same trend, i.e., the higher J for N_2 leads to less rotational activation of $UreaH^+$ and less CID.

Finally, we have shown that the nature of the protonated urea gas phase reactivity is governed by its rotational activation. The fragmentation dynamics were studied using the OPr ↔ NPr transition state as the initial structure, which was excited with different rotational and vibrational energies comparable with those obtained from CID chemical dynamics simulations with Ar and N_2 as the colliding gas. It was found that by increasing the rotational energy of $UreaH^+$ the probability for its high energy fragmentation pathway to form NH_3 is enhanced. As discussed above a state selective effect is found for rotational activation of $UreaH^+$; i.e., as the rotational quantum number J of N_2 is increased, the probability of collisional energy transfer to $UreaH^+$ rotation decreases. In previous experimental studies of ion–molecule collisions state-selection was largely performed for the electronic state of the ion [42], with much less was done on the rotational energy control. Morris and Viggiano have reviewed these studies [43], pointing out that for most reactions rotational temperature has little or no influence on reactivity [44]. An effect can be found in the case of endothermic reactions, where different forms of temperature/energy promote reactivity simply by overcoming the mild reaction endothermicity [45]. This is similar to endothermic fragmentation of NPr isomer where we found that increasing rotational energy we increase its reactivity. For the $HBr^+ + CO_2 \rightarrow HOCO^+ + Br$ reaction in the $^2\Pi_{3/2}$ and $^2\Pi_{1/2}$ states, Weitzel and co-workers [46,47] found that increasing the HBr^+ rotational energy decreased the reaction cross section. This decreased reactivity with HBr^+ rotational energy is similar to our finding of less rotational energy transfer to $UreaH^+$ with increase in N_2 rotational energy.

In conclusion, we have shown that using the diatomic molecule N_2 as the collision gas, instead of Ar, there are differences in CID energy transfer and fragmentation probabilities due to differences in the rotational activation of the ion. This was shown for protonated urea where rotational energy plays an important role in the gas phase fragmentation probability and may be equally important for all cases where rotational activation may determine and guide the ion's unimolecular pathways.

Acknowledgments

This work was granted access to HPC resources under the allocation 2011082123 made by GENCI (Grand Equipement National de Calcul Intensif). KS thanks Université d'Evry Val d'Essonne for a visiting Professor Fellowship and partial support from the Basic Science Program through the National Research Foundation of Korea (KRF) administered by the Ministry of Education, Science and Technology (2011-0008992). The contribution by WLH was performed as part of research supported by the National Science Foundation under Grant No. CHE-0957521 and by the Robert A. Welch Foundation under Grant No. D-0005.

References

[1] R.G. Cooks, in: R.G. Cooks (Ed.), Collision Spectroscopy, Plenum, New York, 1978.
[2] E.R. Fisher, B.L. Kickel, P.B. Armentrout, J. Phys. Chem. 97 (1993) 10204.
[3] R.E. Tosh, A.K. Shukla, J.H. Futrell, J. Chem. Phys. 114 (2986) (2001).
[4] F. Muntean, P.B. Armentrout, J. Chem. Phys. 115 (2001) 1213.
[5] Y.J. Fu, J. Laskin, L.S. Wang, Int. J. Mass Spectrom. 255 (2006) 102.
[6] D.R. Carl, R.M. Moision, P.B. Armentrout, Int. J. Mass Spectrom. 256 (2007) 308.
[7] P.B. Armentrout, H. Koizumi, M. MacKenna, J. Phys. Chem. A 109 (2005) 11365.
[8] J.-Y. Salpin, J. Tortajada, J. Mass Spectrom. 37 (2002) 379.
[9] N. Hallowita, D.R. Carl, P.B. Armentrout, M.T. Rodgers, J. Phys. Chem. A 112 (2008) 7996.
[10] R. Chawla, A. Shukla, J.H. Futrell, J. Phys. Chem. A 105 (2001) 349.
[11] W. Buchmann, R. Spezia, G. Tournois, T. Cartailler, J. Tortajada, J. Mass Spectrom. 42 (2007) 517.

[12] A.L. Heaton, P.B. Armentrout, J. Phys. Chem. A 112 (2008) 10156.
[13] J. Laskin, E. Denisov, J.H. Futrell, Int. J. Mass Spectrom. 219 (2002) 189.
[14] J. Laskin, E. Denisov, J.H. Futrell, J. Chem. Phys. 116 (2002) 4302.
[15] X. Chen, L. Yu, J.D. Steill, J. Oomens, N.C. Polfer, J. Am. Chem. Soc. 131 (2009) 18272.
[16] R. Spezia, J.-Y. Salpin, M.-P. Gaigeot, W.L. Hase, K. Song, J. Phys. Chem. A 113 (2009) 13853.
[17] O. Meroueh, W.L. Hase, J. Phys. Chem. A 103 (1999) 3981.
[18] J. Liu, B.W. Uselman, J.M. Boyle, S.L. Anderson, J. Chem. Phys. 125 (2006) 133115.
[19] L. Sun, W.L. Hase, Rev. Comput. Chem. 19 (2003) 79.
[20] G.H. Peslherbe, H. Wang, W.L. Hase, Adv. Chem. Phys. 105 (1999) 171.
[21] E. Martìnez-Nuñez, A. Fernàndez-Ramos, S.A. Vàzquez, J.M.C. Marques, M. Xue, W.L. Hase, J. Chem. Phys. 123 (2005) 154311.
[22] J. Liu, K. Song, W.L. Hase, S.L. Anderson, J. Chem. Phys. 119 (2003) 3040.
[23] P. de Sainte Claire, W.L. Hase, J. Phys. Chem. 100 (1996) 8190.
[24] R. Spezia, A. Cimas, J.-Y. Salpin, M.-P. Gaigeot, K. Song, W.L. Hase, in preparation.
[25] S.F. Boys, F. Bernardi, Mol. Phys. 19 (1970) 553.
[26] F.M. Tao, Y.K. Pan, J. Phys. Chem. 95 (1991) 3582.
[27] F. Rogalewicz, Y. Hoppilliard, G. Ohanessian, Int. J. Mass Spectrom. 206 (2001) 45.
[28] J.-Y. Salpin, S. Guillaumont, J. Tortajada, L. MacAleese, J. Lemaire, P. Maitre, ChemPhysChem 8 (2007) 2235.
[29] J.M. Bakker, M. Brugnara, T. Besson, J.-Y. Salpin, P.J. Maitre, Phys. Chem. A 112 (2008) 12393.
[30] Y.-P.J. Tu, Org. Chem. 71 (2006) 5482.
[31] S. Chapman, D.L. Bunker, J. Chem. Phys. 62 (2890) (1975).
[32] C.S. Sloane, W.L. Hase, J. Chem. Phys. 66 (1977) 1523.
[33] Y.J. Cho, S.R. Vande Linde, L. Zhu, W.L. Hase, J. Chem. Phys. 96 (1992) 8275.
[34] W.L. Hase, R.J. Duchovic, X. Hu, A. Komornicki, K.F. Lim, D.-h. Lu, G.H. Peslherbe, K.N. Swamy, S.R. Vande Linde, A. Varandas, H. Wang, R.J. Wolf, QCPE 16 (1996) 671.
[35] X. Hu, W.L. Hase, J. Comput. Chem. 12 (1014) (1991).
[36] M.J. Frisch, G.W. Trucks, H.B. Schlegel, G.E. Scuseria, M.A. Robb, J.R. Cheeseman, J.A. Montgomery Jr., T. Vreven, K.N. Kudin, J.C. Burant, J.M. Millam, S.S. Iyengar, J. Tomasi, V. Barone, B. Mennucci, M. Cossi, G. Scalmani, N. Rega, G.A. Petersson, H. Nakatsuji, M. Hada, M. Ehara, K. Toyota, R. Fukuda, J. Hasegawa, M. Ishida, T. Nakajima, Y. Honda, O. Kitao, H. Nakai, M. Klene, X. Li, J.E. Knox, H.P. Hratchian, J.B. Cross, V. Bakken, C. Adamo, J. Jaramillo, R. Gomperts, R.E. Stratmann, O. Yazyev, A.J. Austin, R. Cammi, C. Pomelli, J.W. Ochterski, P.Y. Ayala, K. Morokuma, G.A. Voth, P. Salvador, J.J. Dannenberg, V.G. Zakrzewski, S. Dapprich, A.D. Daniels, M.C. Strain, O. Farkas, D.K. Malick, A.D. Rabuck, K. Raghavachari, J.B. Foresman, J.V. Ortiz, Q. Cui, A.G. Baboul, S. Clifford, J. Cioslowski, B.B. Stefanov, G. Liu, A. Liashenko, P. Piskorz, I. Komaromi, R.L. Martin, D.J. Fox, T. Keith, M.A. Al-Laham, C.Y. Peng, A. Nanayakkara, M. Challacombe, P.M.W. Gill, B. Johnson, W. Chen, M.W. Wong, C. Gonzalez, J.A. Pople, Gaussian 03, Revision D.01, Gaussian, Inc., Wallingford, CT, 2004.
[37] W.C. Swope, H.C. Andersen, P.H. Berens, K.R. Wilson, J. Chem. Phys. 76 (1982) 637.
[38] W.L. Hase, D.G. Buckowski, Chem. Phys. Lett. 74 (1980) 284.
[39] O. Meroueh, W.L. Hase, Int. J. Mass Spectrom. 201 (2000) 233.
[40] P. de Sainte Claire, G.H. Peslherbe, W.L. Hase, J. Phys. Chem. 99 (1995) 8147.
[41] B.H.J. Mahan, Chem. Phys. 52 (1970) 5221.
[42] C.-Y.J. Ng, Phys. Chem. A 106 (2002) 5953.
[43] A.A. Viggiano, R.A. Morris, J. Phys. Chem. 100 (1996) 19227.
[44] I. Dotan, A.A. Viggiano, Chem. Phys. Lett. 209 (1993) 67.
[45] A.A. Viggiano, R.A. Morris, F. Dale, J.F. Paulson, K. Giles, D. Smith, T. Su, J. Chem. Phys. 93 (1990) 1149.
[46] L. Paetow, F. Unger, B. Beutel, K.-M. Weitzel, J. Chem. Phys. 133 (2010) 234301.
[47] L. Paetow, F. Unger, W. Beichel, G. Frenking, K.-M. Weitzel, J. Chem. Phys. 132 (2010) 174305.